EUROPEAN ORGANIZATION FOR NUCLEAR RESEARCH

CERN–PPE/95-91

23 June 1995

Search for exclusive charmless B meson decays with the DELPHI detector at LEP

DELPHI Collaboration

Abstract

Charmless hadronic decays of beauty mesons have been searched for using the data collected with the DELPHI detector at the LEP collider. Several two, three and four-body decay modes have been investigated. Particle identification was used to distinguish the final states with protons, kaons and pions. Three candidate events selected in two-body decay modes are interpreted as evidence for charmless B decays. No excess has been found in higher multiplicity modes and improved upper limits for some of the branching ratios are given.

(To be submitted to Physics Letters B)

P.Abreu[21], W.Adam[50], T.Adye[37], E.Agasi[31], I.Ajinenko[42], R.Aleksan[39], G.D.Alekseev[16], P.P.Allport[22], S.Almehed[24], S.J.Alvsvaag[4], U.Amaldi[9], S.Amato[47], A.Andreazza[28], M.L.Andrieux[14], P.Antilogus[25], W-D.Apel[17], Y.Arnoud[39], B.Åsman[44], J-E.Augustin[19], A.Augustinus[31], P.Baillon[9], P.Bambade[19], F.Barao[21], R.Barate[14], G.Barbiellini[46], D.Y.Bardin[16], G.J.Barker[35], A.Baroncelli[40], O.Barring[24], J.A.Barrio[26], W.Bartl[50], M.J.Bates[37], M.Battaglia[15], M.Baubillier[23], J.Baudot[39], K-H.Becks[52], M.Begalli[6], P.Beilliere[8], Yu.Belokopytov[9], A.C.Benvenuti[5], M.Berggren[47], D.Bertrand[2], F.Bianchi[45], M.Bigi[45], M.S.Bilenky[16], P.Billoir[23], D.Bloch[10], M.Blume[52], S.Blyth[35], V.Bocci[38], T.Bolognese[39], M.Bonesini[28], W.Bonivento[28], P.S.L.Booth[22], G.Borisov[42], C.Bosio[40], S.Bosworth[35], O.Botner[48], E.Boudinov[42], B.Bouquet[19], C.Bourdarios[9], T.J.V.Bowcock[22], M.Bozzo[13], P.Branchini[40], K.D.Brand[36], T.Brenke[52], R.A.Brenner[15], C.Bricman[2], L.Brillault[23], R.C.A.Brown[9], P.Bruckman[18], J-M.Brunet[8], L.Bugge[33], T.Buran[33], T.Burgsmueller[52], P.Buschmann[52], A.Buys[9], M.Caccia[28], M.Calvi[28], A.J.Camacho Rozas[41], T.Camporesi[9], V.Canale[38], M.Canepa[13], K.Cankocak[44], F.Cao[2], F.Carena[9], P.Carrilho[47], L.Carroll[22], C.Caso[13], M.V.Castillo Gimenez[49], A.Cattai[9], F.R.Cavallo[5], L.Cerrito[38], V.Chabaud[9], Ph.Charpentier[9], L.Chaussard[25], J.Chauveau[23], P.Checchia[36], G.A.Chelkov[16], R.Chierici[45], P.Chliapnikov[42], P.Chochula[7], V.Chorowicz[9], V.Cindro[43], P.Collins[9], J.L.Contreras[19], R.Contri[13], E.Cortina[49], G.Cosme[19], F.Cossutti[46], H.B.Crawley[1], D.Crennell[37], G.Crosetti[13], J.Cuevas Maestro[34], S.Czellar[15], E.Dahl-Jensen[29], J.Dahm[52], B.Dalmagne[19], M.Dam[33], G.Damgaard[29], A.Daum[17], P.D.Dauncey[37], M.Davenport[9], W.Da Silva[23], C.Defoix[8], G.Della Ricca[46], P.Delpierre[27], N.Demaria[35], A.De Angelis[9], H.De Boeck[2], W.De Boer[17], S.De Brabandere[2], C.De Clercq[2], C.De La Vaissiere[23], B.De Lotto[46], A.De Min[28], L.De Paula[47], C.De Saint-Jean[39], H.Dijkstra[9], L.Di Ciaccio[38], F.Djama[10], J.Dolbeau[8], M.Donszelmann[9], K.Doroba[51], M.Dracos[10], J.Drees[52], K.-A.Drees[52], M.Dris[32], Y.Dufour[8], F.Dupont[14], D.Edsall[1], R.Ehret[17], G.Eigen[4], T.Ekelof[48], G.Ekspong[44], M.Elsing[52], J-P.Engel[10], N.Ershaidat[23], B.Erzen[43], M.Espirito Santo[21], E.Falk[24], D.Fassouliotis[32], M.Feindt[9], A.Ferrer[49], T.A.Filippas[32], A.Firestone[1], P.-A.Fischer[10], H.Foeth[9], E.Fokitis[32], F.Fontanelli[13], F.Formenti[9], B.Franek[37], P.Frenkiel[8], D.C.Fries[17], A.G.Frodesen[4], R.Fruhwirth[50], F.Fulda-Quenzer[19], H.Furstenau[9], J.Fuster[49], A.Galloni[22], D.Gamba[45], M.Gandelman[6], C.Garcia[49], J.Garcia[41], C.Gaspar[9], U.Gasparini[36], Ph.Gavillet[9], E.N.Gazis[32], D.Gele[10], J-P.Gerber[10], L.Gerdyukov[42], M.Gibbs[22], D.Gillespie[9], R.Gokieli[51], B.Golob[43], G.Gopal[37], L.Gorn[1], M.Gorski[51], Yu.Gouz[42], V.Gracco[13], E.Graziani[40], G.Grosdidier[19], P.Gunnarsson[44], M.Gunther[48], J.Guy[37], U.Haedinger[17], F.Hahn[9], M.Hahn[17], S.Hahn[52], Z.Hajduk[18], A.Hallgren[48], K.Hamacher[52], W.Hao[31], F.J.Harris[35], V.Hedberg[24], R.Henriques[21], J.J.Hernandez[49], P.Herquet[2], H.Herr[9], T.L.Hessing[9], E.Higon[49], H.J.Hilke[9], T.S.Hill[1], S-O.Holmgren[44], P.J.Holt[35], D.Holthuizen[31], M.Houlden[22], J.Hrubec[50], K.Huet[2], K.Hultqvist[44], P.Ioannou[3], J.N.Jackson[22], R.Jacobsson[44], P.Jalocha[18], R.Janik[7], G.Jarlskog[24], P.Jarry[39], B.Jean-Marie[19], E.K.Johansson[44], L.Jonsson[24], P.Jonsson[24], C.Joram[9], P.Juillot[10], M.Kaiser[17], G.Kalmus[37], F.Kapusta[23], M.Karlsson[44], E.Karvelas[11], S.Katsanevas[3], E.C.Katsoufis[32], R.Keranen[15], B.A.Khomenko[16], N.N.Khovanski[16], B.King[22], N.J.Kjaer[29], H.Klein[9], A.Klovning[4], P.Kluit[31], J.H.Koehne[17], B.Koene[31], P.Kokkinias[11], M.Koratzinos[9], V.Kostioukhine[42], C.Kourkoumelis[3], O.Kouznetsov[13], P.-H.Kramer[52], M.Krammer[50], C.Kreuter[17], J.Krolikowski[51], I.Kronkvist[24], Z.Krumstein[16], W.Krupinski[18], P.Kubinec[7], W.Kucewicz[18], K.Kurvinen[15], C.Lacasta[49], I.Laktineh[25], S.Lamblot[23], J.W.Lamsa[1], L.Lanceri[46], D.W.Lane[1], P.Langefeld[52], I.Last[22], J-P.Laugier[39], R.Lauhakangas[15], G.Leder[50], F.Ledroit[14], V.Lefebure[2], C.K.Legan[1], R.Leitner[30], Y.Lemoigne[39], J.Lemonne[2], G.Lenzen[52], V.Lepeltier[19], T.Lesiak[36], D.Liko[50], R.Lindner[52], A.Lipniacka[19], I.Lippi[36], B.Loerstad[24], M.Lokajicek[12], J.G.Loken[35], J.M.Lopez[41], A.Lopez-Fernandez[9], M.A.Lopez Aguera[41], D.Loukas[11], P.Lutz[39], L.Lyons[35], J.MacNaughton[50], G.Maehlum[17], V.Malychev[16], F.Mandl[50], J.Marco[41], B.Marechal[47], M.Margoni[36], J-C.Marin[9], C.Mariotti[40], A.Markou[11], T.Maron[52], C.Martinez-Rivero[41], F.Martinez-Vidal[49], S.Marti i Garcia[49], F.Matorras[41], C.Matteuzzi[28], G.Matthiae[38], M.Mazzucato[36], M.Mc Cubbin[9], R.Mc Kay[1], R.Mc Nulty[22], J.Medbo[48], C.Meroni[28], W.T.Meyer[1], M.Michelotto[36], E.Migliore[45], L.Mirabito[25], W.A.Mitaroff[50], U.Mjoernmark[24], T.Moa[44], R.Moeller[29], K.Moenig[9], M.R.Monge[13], P.Morettini[13], H.Mueller[17], L.M.Mundim[6], W.J.Murray[37], B.Muryn[18], G.Myatt[35], F.Naraghi[14], F.L.Navarria[5], S.Navas[49], P.Negri[28], S.Nemecek[12], W.Neumann[52], N.Neumeister[50], R.Nicolaidou[3], B.S.Nielsen[29], M.Nieuwenhuizen[31], V.Nikolaenko[10], P.Niss[44], A.Nomerotski[36], A.Normand[35], W.Oberschulte-Beckmann[17], V.Obraztsov[42], A.G.Olshevski[16], A.Onofre[21], R.Orava[15], K.Osterberg[15], A.Ouraou[39], P.Paganini[19], M.Paganoni[28], P.Pages[10], H.Palka[18], Th.D.Papadopoulou[32], L.Pape[9], C.Parkes[35], F.Parodi[13], A.Passeri[40], M.Pegoraro[36], L.Peralta[21], H.Pernegger[50], M.Pernicka[50], A.Perrotta[5], C.Petridou[46], A.Petrolini[13], H.T.Phillips[37], G.Piana[13], F.Pierre[39], M.Pimenta[21], S.Plaszczynski[19], O.Podobrin[17], M.E.Pol[6], G.Polok[18], P.Poropat[46], V.Pozdniakov[16], M.Prest[46], P.Privitera[38], N.Pukhaeva[16], A.Pullia[28], D.Radojicic[35], S.Ragazzi[28], H.Rahmani[32], J.Rames[12], P.N.Ratoff[20], A.L.Read[33], M.Reale[52], P.Rebecchi[19], N.G.Redaelli[28], M.Regler[50], D.Reid[9], P.B.Renton[35], L.K.Resvanis[3], F.Richard[19], J.Richardson[22], J.Ridky[12], G.Rinaudo[45], I.Ripp[39], A.Romero[45], I.Roncagliolo[13], P.Ronchese[36], L.Roos[14], E.I.Rosenberg[1], E.Rosso[9], P.Roudeau[19], T.Rovelli[5], W.Ruckstuhl[31], V.Ruhlmann-Kleider[39], A.Ruiz[41], H.Saarikko[15], Y.Sacquin[39], A.Sadovsky[16], G.Sajot[14], J.Salt[49], J.Sanchez[26], M.Sannino[13], H.Schneider[17], M.A.E.Schyns[52], G.Sciolla[45], F.Scuri[46], Y.Sedykh[16], A.M.Segar[35], A.Seitz[17], R.Sekulin[37], R.C.Shellard[6], I.Siccama[31], P.Siegrist[39], S.Simonetti[39], F.Simonetto[36], A.N.Sisakian[16], B.Sitar[7], T.B.Skaali[33], G.Smadja[25], N.Smirnov[42], O.Smirnova[16], G.R.Smith[37], A.Sokolov[42], O.Solovyanov[42], R.Sosnowski[51], D.Souza-Santos[6], T.Spassov[21], E.Spiriti[40], P.Sponholz[52], S.Squarcia[13], C.Stanescu[40], S.Stapnes[33], I.Stavitski[36], K.Stepaniak[51], F.Stichelbaut[9], A.Stocchi[19], J.Strauss[50], R.Strub[10], B.Stugu[4], M.Szczekowski[51], M.Szeptycka[51], T.Tabarelli[28], J.P.Tavernet[23], O.Tchikilev[42],

A.Tilquin[27], J.Timmermans[31], L.G.Tkatchev[16], T.Todorov[10], D.Z.Toet[31], A.Tomaradze[2], B.Tome[21], L.Tortora[40], G.Transtromer[24], D.Treille[9], W.Trischuk[9], G.Tristram[8], A.Trombini[19], C.Troncon[28], A.Tsirou[9], M-L.Turluer[39], I.A.Tyapkin[16], M.Tyndel[37], S.Tzamarias[22], B.Ueberschaer[52], O.Ullaland[9], V.Uvarov[42], G.Valenti[5], E.Vallazza[9], C.Vander Velde[2], G.W.Van Apeldoorn[31], P.Van Dam[31], W.K.Van Doninck[2], J.Van Eldik[31], N.Vassilopoulos[35], G.Vegni[28], L.Ventura[36], W.Venus[37], F.Verbeure[2], M.Verlato[36], L.S.Vertogradov[16], D.Vilanova[39], P.Vincent[25], L.Vitale[46], E.Vlasov[42], A.S.Vodopyanov[16], V.Vrba[12], H.Wahlen[52], C.Walck[44], M.Weierstall[52], P.Weilhammer[9], A.M.Wetherell[9], D.Wicke[52], J.H.Wickens[2], M.Wielers[17], G.R.Wilkinson[35], W.S.C.Williams[35], M.Winter[10], M.Witek[9], K.Woschnagg[48], K.Yip[35], O.Yushchenko[42], F.Zach[25], C.Zacharatou[24], A.Zalewska[18], P.Zalewski[51], D.Zavrtanik[43], E.Zevgolatakos[11], N.I.Zimin[16], M.Zito[39], D.Zontar[43], R.Zuberi[35], G.C.Zucchelli[44], G.Zumerle[36]

[1] Ames Laboratory and Department of Physics, Iowa State University, Ames IA 50011, USA
[2] Physics Department, Univ. Instelling Antwerpen, Universiteitsplein 1, B-2610 Wilrijk, Belgium
and IIHE, ULB-VUB, Pleinlaan 2, B-1050 Brussels, Belgium
and Faculté des Sciences, Univ. de l'Etat Mons, Av. Maistriau 19, B-7000 Mons, Belgium
[3] Physics Laboratory, University of Athens, Solonos Str. 104, GR-10680 Athens, Greece
[4] Department of Physics, University of Bergen, Allégaten 55, N-5007 Bergen, Norway
[5] Dipartimento di Fisica, Università di Bologna and INFN, Via Irnerio 46, I-40126 Bologna, Italy
[6] Centro Brasileiro de Pesquisas Físicas, rua Xavier Sigaud 150, RJ-22290 Rio de Janeiro, Brazil
and Depto. de Física, Pont. Univ. Católica, C.P. 38071 RJ-22453 Rio de Janeiro, Brazil
and Inst. de Física, Univ. Estadual do Rio de Janeiro, rua São Francisco Xavier 524, Rio de Janeiro, Brazil
[7] Comenius University, Faculty of Mathematics and Physics, Mlynska Dolina, SK-84215 Bratislava, Slovakia
[8] Collège de France, Lab. de Physique Corpusculaire, IN2P3-CNRS, F-75231 Paris Cedex 05, France
[9] CERN, CH-1211 Geneva 23, Switzerland
[10] Centre de Recherche Nucléaire, IN2P3 - CNRS/ULP - BP20, F-67037 Strasbourg Cedex, France
[11] Institute of Nuclear Physics, N.C.S.R. Demokritos, P.O. Box 60228, GR-15310 Athens, Greece
[12] FZU, Inst. of Physics of the C.A.S. High Energy Physics Division, Na Slovance 2, 180 40, Praha 8, Czech Republic
[13] Dipartimento di Fisica, Università di Genova and INFN, Via Dodecaneso 33, I-16146 Genova, Italy
[14] Institut des Sciences Nucléaires, IN2P3-CNRS, Université de Grenoble 1, F-38026 Grenoble Cedex, France
[15] Research Institute for High Energy Physics, SEFT, P.O. Box 9, FIN-00014 Helsinki, Finland
[16] Joint Institute for Nuclear Research, Dubna, Head Post Office, P.O. Box 79, 101 000 Moscow, Russian Federation
[17] Institut für Experimentelle Kernphysik, Universität Karlsruhe, Postfach 6980, D-76128 Karlsruhe, Germany
[18] High Energy Physics Laboratory, Institute of Nuclear Physics, Ul. Kawiory 26a, PL-30055 Krakow 30, Poland
[19] Université de Paris-Sud, Lab. de l'Accélérateur Linéaire, IN2P3-CNRS, Bât. 200, F-91405 Orsay Cedex, France
[20] School of Physics and Materials, University of Lancaster, Lancaster LA1 4YB, UK
[21] LIP, IST, FCUL - Av. Elias Garcia, 14-1^{o}, P-1000 Lisboa Codex, Portugal
[22] Department of Physics, University of Liverpool, P.O. Box 147, Liverpool L69 3BX, UK
[23] LPNHE, IN2P3-CNRS, Universités Paris VI et VII, Tour 33 (RdC), 4 place Jussieu, F-75252 Paris Cedex 05, France
[24] Department of Physics, University of Lund, Sölvegatan 14, S-22363 Lund, Sweden
[25] Université Claude Bernard de Lyon, IPNL, IN2P3-CNRS, F-69622 Villeurbanne Cedex, France
[26] Universidad Complutense, Avda. Complutense s/n, E-28040 Madrid, Spain
[27] Univ. d'Aix - Marseille II - CPP, IN2P3-CNRS, F-13288 Marseille Cedex 09, France
[28] Dipartimento di Fisica, Università di Milano and INFN, Via Celoria 16, I-20133 Milan, Italy
[29] Niels Bohr Institute, Blegdamsvej 17, DK-2100 Copenhagen 0, Denmark
[30] NC, Nuclear Centre of MFF, Charles University, Areal MFF, V Holesovickach 2, 180 00, Praha 8, Czech Republic
[31] NIKHEF-H, Postbus 41882, NL-1009 DB Amsterdam, The Netherlands
[32] National Technical University, Physics Department, Zografou Campus, GR-15773 Athens, Greece
[33] Physics Department, University of Oslo, Blindern, N-1000 Oslo 3, Norway
[34] Dpto. Fisica, Univ. Oviedo, C/P. Pérez Casas, S/N-33006 Oviedo, Spain
[35] Department of Physics, University of Oxford, Keble Road, Oxford OX1 3RH, UK
[36] Dipartimento di Fisica, Università di Padova and INFN, Via Marzolo 8, I-35131 Padua, Italy
[37] Rutherford Appleton Laboratory, Chilton, Didcot OX11 OQX, UK
[38] Dipartimento di Fisica, Università di Roma II and INFN, Tor Vergata, I-00173 Rome, Italy
[39] Centre d'Etudes de Saclay, DSM/DAPNIA, F-91191 Gif-sur-Yvette Cedex, France
[40] Istituto Superiore di Sanità, Ist. Naz. di Fisica Nucl. (INFN), Viale Regina Elena 299, I-00161 Rome, Italy
[41] C.E.A.F.M., C.S.I.C. - Univ. Cantabria, Avda. los Castros, S/N-39006 Santander, Spain, (CICYT-AEN93-0832)
[42] Inst. for High Energy Physics, Serpukov P.O. Box 35, Protvino, (Moscow Region), Russian Federation
[43] J. Stefan Institute and Department of Physics, University of Ljubljana, Jamova 39, SI-61000 Ljubljana, Slovenia
[44] Fysikum, Stockholm University, Box 6730, S-113 85 Stockholm, Sweden
[45] Dipartimento di Fisica Sperimentale, Università di Torino and INFN, Via P. Giuria 1, I-10125 Turin, Italy
[46] Dipartimento di Fisica, Università di Trieste and INFN, Via A. Valerio 2, I-34127 Trieste, Italy
and Istituto di Fisica, Università di Udine, I-33100 Udine, Italy
[47] Univ. Federal do Rio de Janeiro, C.P. 68528 Cidade Univ., Ilha do Fundão BR-21945-970 Rio de Janeiro, Brazil
[48] Department of Radiation Sciences, University of Uppsala, P.O. Box 535, S-751 21 Uppsala, Sweden
[49] IFIC, Valencia-CSIC, and D.F.A.M.N., U. de Valencia, Avda. Dr. Moliner 50, E-46100 Burjassot (Valencia), Spain
[50] Institut für Hochenergiephysik, Österr. Akad. d. Wissensch., Nikolsdorfergasse 18, A-1050 Vienna, Austria
[51] Inst. Nuclear Studies and University of Warsaw, Ul. Hoza 69, PL-00681 Warsaw, Poland
[52] Fachbereich Physik, University of Wuppertal, Postfach 100 127, D-42097 Wuppertal 1, Germany

1 Introduction

Charmless hadronic decays of beauty mesons can occur both through tree level diagrams involving $b \to u$ transitions and loop diagrams known as "hadronic penguin" diagrams (see figure 1). These decays have been the subject of considerable interest. Tree level dominated decays confirm the non-zero value of $|V_{ub}|$ in the CKM mixing matrix while those induced by penguin processes provide tests of the loop structure of the Standard Model. Branching ratios for a large number of two-body exclusive decay modes have been predicted and are in the range of $(0.1-1.8)\times 10^{-4}$[1–4]. Evidence for charmless decays has been reported by the CLEO collaboration which has obtained signals for both the radiative decay $B \to K^*\gamma$ [5] and the two body hadronic decays $B \to \pi\ (K)\ \pi$ [6]. At present it is important to confirm the existence of these decays in two body modes, and to extend the search to as wide a variety of channels as possible. When more data become available, it may be possible to study the interference of the penguin and tree level amplitudes in hadronic charmless B decays, thereby providing a means to analyze the final state strong interactions [7]. Charmless final states may also originate from rescattering through double charm production. These decays are of special relevance for the studies and the interpretation of CP asymmetries in B decays. Multi-body charmless decays are subject to larger uncertainties both in their theoretical predictions [8] and for the looser constraints provided so far by experimental data. However hadronic charmless b decays are expected to have a large pion multiplicity both when induced by $b \to u$ [9] and by $b \to s$ [10] transitions. This makes the $n\pi$ $(n > 2)$ and $Km\pi$ with $(m > 1)$ final states particularly sensitive to charmless b decays compared to $\pi\pi$ and $K\pi$.

With the statistics presently available at LEP, B branching ratios of a few times 10^{-5} are becoming accessible [11]. There are several advantages in their study at this centre of mass energy. As the B particles have a large fraction of the available energy, their decay products are confined in collimated jets and originate from detached secondary vertices. This feature, when exploited by the use of a silicon vertex detector, allows an effective separation of the particles from the decay of the B particles from those produced in the fragmentation or in light quark events. Further, the particle identification capabilities of the DELPHI detector allow exclusive decay channels with strange particles or protons in the final state to be studied.

This analysis searched for charmless hadronic decays of B mesons in several decay modes with all charged mesons $n\pi$ $(n = 2\ to\ 4)$, nK and $Km\pi$ $(n = 2\ to\ 3;\ m = 1\ to\ 3)$ final states and with baryons $p\bar{p}m\pi$ $(m = 0\ to\ 2)$.

2 Data analysis

The present analysis is based on the statistics collected during 1991, 1992 and 1993 by DELPHI at LEP, corresponding to about 1.7 million Z^0 hadronic decays.

The DELPHI detector has been described elsewhere [12]. Of particular importance for this study are the accurate track extrapolation and the particle identification.

A three layer silicon vertex detector (VD) in the DELPHI tracking system ensures precise track reconstruction near the interaction region. The accuracy of extrapolation for high momentum particle tracks to the vertex was measured to be 24 μm in the transverse plane ($R\phi$). This allows the use of secondary vertex reconstruction to separate B decay products from primary hadronization particles.

Particle identification over a large momentum range is an important feature of the DELPHI detector. Hadrons were identified by the combined use of the information de-

rived from the specific ionisation in the Time Projection Chamber (TPC) and from the Ring Imaging Cherenkov detector (RICH). The TPC provides up to 192 sampling points along the track and a dE/dx resolution of about 7% in hadronic events. This corresponds to separating kaons from pions by 1.5 standard deviations (σ) for particles with momenta above 3.5 GeV/c. The use of the RICH gas radiator separates light particles (e, μ, π) from heavy ones (K, p) above 3.5 GeV/c and gives exclusive kaon and proton identification from 9 to about 20 GeV/c. The identification algorithm used in this analysis was tuned in order to optimise its efficiency. The efficiency for tagging a particle in this kinematical region is about 80 % and independent of the particle momentum. For particles tagged as kaons, the rejection factor against misidentified pions is close to 5 using the dE/dx information and between 8 and 5, depending on the particle momentum, using the RICH detector. In order to increase the efficiency for reconstructing decays with $p\bar{p}$, only the more energetic of the two particles was required to be identified as a proton. The second was only required to be tagged as a heavy particle with momentum above 3.5 GeV/c.

Muon identification was based on the information from the Muon Chambers and the energy deposited in the Hadron Calorimeter. Electrons were tagged by the shape and energy of the associated electromagnetic shower in the High density Projection Chamber (HPC). The dE/dx and RICH information was also used to complement the HPC response for electron tagging.

Identified particles were attributed their corresponding masses. Those without identification information were assumed to be pions.

2.1 Event selection and B decay reconstruction

Hadronic events were selected by the standard Delphi hadronic criteria [13]. These provided 1.62 million events from the combined 1991-1993 data sample. For each event the primary vertex was fitted using a procedure that iteratively linked tracks to the beam-spot. Tracks not compatible with the hypothesis of originating from a common vertex were then removed. The selected hadronic events were divided into two hemispheres defined by the plane perpendicular to the event thrust axis. For each hemisphere the leading charged particle was used to start the secondary vertex reconstruction. The other charged particles were iteratively tested to form a common n-prong detached vertex with this leading particle. These were selected within the $(n + 1)$ most energetic charged particles, which had momenta above 0.8 GeV/c and were within 1.0 rad of the leading track. In order to preserve an accurate extrapolation to the vertex region, only tracks with at least one hit in the VD were considered. The impact parameters for particle tracks were computed in the $R\phi$ plane with respect to the primary vertex. Tracks having impact parameters larger than 0.5 cm were rejected, because they could be due to a long-lived particle decay or to a problem in the pattern recognition. Vertices with a fit probability below 10^{-5} were discarded. Secondary vertices with one or more lepton candidates were also rejected as the lepton comes from either a semileptonic heavy quark decay or a charmonium decay.

Kinematic cuts were applied to exploit the hard b fragmentation. The total energy of the B candidate was required to be larger than 20 GeV and not to exceed the beam energy. For two (greater than two) prong topologies, the momentum of the leading track had to be larger than 10 (8) GeV/c and that of the other secondary tracks larger than 1.0 (0.8) GeV/c.

There are two main sources of background in the reconstruction of exclusive B decays. The first comes from combinatorial background and originates from all Z^0 hadronic de-

cays. This component was suppressed by requiring that the candidate secondary vertex is separated by more than 2.5 σ from the reconstructed primary vertex in the $R\phi$ plane and that the decay distance was smaller than 2.0 cm. This second cut removes background from long-lived particles. In addition a b-tagging algorithm was applied to enhance the fraction of $b\bar{b}$ events in the selected sample. This algorithm used the impact parameter significance of all the tracks in the event and gave the probability P_{prim} for the hypothesis that all particles originate at the Z^0 production point [14]. Events with P_{prim} below 0.15 were selected. In a simulated $q\bar{q}$ sample this criterion selected 65% of $b\bar{b}$ and 15% of non $b\bar{b}$ events.

The second source of background is due to partially reconstructed B decays. This gives a mass distribution that falls steeply up to about 5.0 GeV/c^2 for B mesons. Above this mass value, a rather flat tail extending to much higher masses is present. While partially reconstructed decays of beauty baryons also contribute below the Λ_b mass value, this tail is due mainly to tracks from the primary vertex being incorrectly assigned to the secondary vertex. It was suppressed by requiring every track used in the secondary vertex reconstruction to have an impact parameter with respect to the primary vertex larger than 1.5 times its associated error. Furthermore cuts on the vertex topology were applied. A candidate was rejected if any track not used in the secondary vertex reconstruction either missed the primary vertex by more than 2 σ or fitted the secondary vertex within 1 σ.

These criteria selected a pure sample of secondary vertices from b particle decays. A detailed simulation study showed that 99%, 98% and 94% of the selected two, three and four-prong vertices with invariant mass above 4.5 GeV/c^2 belong to beauty decays and respectively 2%, 12% and 32% of these have one or more primary particles wrongly assigned to the secondary vertex.

2.2 Two-prong topology

The two-prong topology is particularly clean since there is almost no physical source of background in the B mass region. A study of simulated b events including full detector simulation showed that the highest invariant mass obtained by B decay products passing the two-prong selection used in the present analysis and originating from $b \to c$ decay channels is around 4.8 GeV/c^2.

2.3 Multi-prong topologies

In these topologies, fully reconstructed B decays with charmed intermediate states, such as $B \to \psi K n\pi$ and $B \to D n\pi$, have to be rejected. These were removed by requiring that no pair of particles had an invariant mass close to the ψ mass if given electron or muon mass, or close to the D^0 if assigned either kaon-pion or pion-pion masses. The widths of the invariant mass intervals around the charm states corresponded to a 3 σ cut, using the measured mass resolutions of the states considered. Triplets of particles from the four-prong vertices were checked also for compatibility with the D^- mass by testing all the possible $K^-\pi^+\pi^-$ mass combinations, with the D_s^- mass by testing all possible $K^+K^-\pi^-$ combinations. Again events were removed accordingly. All possible combinations of mass assignments were tested provided the corresponding invariant mass of the multi-prong was compatible with the B mass region defined below. The efficiency of these criteria in rejecting beauty decays to charm has been evaluated with simulation by studying the fractions of rejected events, for which all the tracks used at the secondary vertex came

from a $b \to c$ decay. These fractions were (94 ± 3) % and (96 ± 2) % for three and four-prong topology respectively. A further suppression of the charm intermediate states was achieved by the application of particle identification requirements and intermediate resonance constraints depending on the channel considered. The charm states passing the selection criteria were taken into account in the evaluation of the background.

Charmless b decays were classified in the following way. A decay was considered to take place via an intermediate resonance provided that the reconstructed mass of the relevant particles was within 2 σ of the resonance mass, where σ is the convolution of the natural width and the mass resolution, and the mass assignments were consistent with the particle identification information. For $\phi \to KK$ only one of the two kaons had to be identified, since the narrow mass cut around the ϕ mass already efficiently removed most of the combinatorial background. In the B decays involving a vector and a pseudo-scalar meson, such as $B \to K^*\pi$ and $\rho\pi$, the vector meson is fully polarized. The distribution of events as a function of the helicity angle θ^* in the vector meson rest frame is proportional to $\cos^2\theta^*$ while the background is more isotropic. Therefore in these channels $|\cos\theta^*|$ was required to be larger than 0.5.

2.4 Efficiency and background evaluation

Reconstruction efficiencies were evaluated using Monte Carlo generated samples of signal events passed through full detector simulation. The mass resolution was found to be (90 ± 6) MeV/c^2 for the two-prong, (61 ± 5) MeV/c^2 for three-prong and (45 ± 8) MeV/c^2 for four-prong topology. The $B_{d,u}$ (B_s) candidates were accepted in the invariant mass region defined by the intervals $5.15 - 5.55$ GeV/c^2 ($5.25 - 5.65$ GeV/c^2) and $5.20 - 5.50$ GeV/c^2 ($5.30 - 5.60$ GeV/c^2) for two and more than two-prongs respectively.

Efficiencies were studied in two steps. First the effect of the cuts described above on the signal sample was evaluated. The efficiency was found to be 16% for the two-prongs, 6% for the three-prongs and 4% for the four-prongs. In the second step, the efficiency for the particle identification and for the cuts on the intermediate mass states was measured for each specific channel. As the sample of identified kaons is rather pure and most of the two body channels considered include intermediate resonances, the mis-classification probability is small. Assuming equal production rate, only 10% of the events classified as $\pi\pi$ come from misidentified $K\pi$ signal events and only 4% of those reconstructed as $K^*\pi$ and $\rho\pi$ are from non-resonant three body decays.

The background was studied with three samples of simulated events: 2.95 million $q\bar{q}$ events, 1.05 million $b\bar{b}$ events and 0.25 million $c\bar{c}$ events. This simulated sample corresponds to about 4.6 times the amount of real data. The decay branching ratios for beauty mesons in the simulation were tuned in order to reproduce the present data on exclusive channels and inclusive particle content and kinematics. For the beauty baryons the experimental data are still very limited. Therefore the results of the fragmentation and decays as treated in the JETSET program [15] were assumed. The uncertainty in the b baryon production and decay was included as a source of systematic error in the evaluation of the background. Charmless b decays were removed for evaluating the backgrounds. The rejection factors of the cuts at each stage of the selection were compared for real and simulated data and found to be in good agreement. Finally absolute normalizations corresponding to the number of selected hadronic Z^0 decays in each quark state were applied to the simulated data.

Special samples of beauty meson and baryon decays in a number of exclusive channels were also used to study the possible contamination from $b \to c$ decays in the multi-prong modes.

3 Results and discussion

The individual channels studied for the different decay modes are discussed in this section. Upper limits at 90% confidence level for the branching ratio of these channels are derived. In computing these limits, the fractions of $B^{0,-}_{d,u}$ and B^0_s mesons were assumed to be 0.39 and 0.12 respectively. Several channels can receive contributions from decays of both the B^0_d and B^0_s mesons. Since these contributions cannot be separated with the present statistics and mass resolution, limits are given for the weighted average of the decay rates of the two neutral B mesons.

The number of background events expected in the signal region was evaluated in two ways. The first estimate used the number of events found in the simulation samples in the mass region from 5.1 GeV/c^2 to 6.0 GeV/c^2 normalised to the signal mass interval. As a second method, the background was evaluated for each individual channel by studying independently the rejection powers of the cuts applied. The secondary vertex selection criteria were relaxed for the two-prong sample. The effect of intermediate mass and the helicity angle constraints were also studied in the multi-prong sample. In addition the background suppression coming from kaon or proton identification was measured for all the channels. This second method reduces the statistical uncertainty on the estimate. However it assumes that the effects of the cuts are independent. Its reliability was therefore further checked by comparing the number of events seen in the real data for all the channels considered in this analysis with the expected number of events in the mass interval from 4.95 GeV/c^2 to 6.0 GeV/c^2 but excluding the signal regions. Summing over all the decay modes considered in the present analysis, the number of events expected from the study of the rejection powers in simulation was 21.3 ± 1.0, in good agreement with 18 events present in the data. For comparison the expected number of events obtained with the first method by counting the events passing all the cuts in the simulation sample was 17.2 ± 2.0.

3.1 Two body decay modes

The following decay modes and their corresponding charge conjugates were investigated:

- $B^0_d \to \pi^+\pi^-$
- $B^-_u \to \rho(770)^0\pi^-, \quad \rho(770)^0 \to \pi^+\pi^-$
- $B^0_{d,s} \to K^+\pi^-$
- $B^-_u \to K^-\rho(770)^0, \quad \rho(770)^0 \to \pi^+\pi^-$
- $B^0_{d,s} \to K^+a_1(1270)^-, \quad a_1(1270)^- \to \pi^-\pi^+\pi^-$
- $B^-_u \to \bar{K}^*(892)^0\pi^-, \quad \bar{K}^*(892)^0 \to K^-\pi^+$
- $B^0_{d,s} \to K^+K^-$
- $B^-_u \to \phi(1020)K^-, \quad \phi(1020) \to K^+K^-$
- $B^0_d \to p\bar{p}$

Three candidate events were found in the mass intervals defining the signal region close to the B mass. They are in the $B^0_{d,s} \to K^+\pi^-$, $B^-_u \to \rho(770)^0\pi^-$ and $B^-_u \to \bar{K}^*(892)^0\pi^-$

channels. In the first event the kaon was identified only in the TPC, in the last it was identified using both the RICH and TPC. In table 1 the reconstructed mass of the candidates, their energy E_B, the significance of their decay distance d and the proper decay time τ_B are given. For the two decay candidates including a resonant state, also the values for $|cos\theta^*|$ and the distance from the central value of the mass of the resonance in units of its total r.m.s. are given. A display of the vertex region for the $K^*\pi$ candidate is shown in figure 2 together with the hadron identification properties.

Table 1: Characteristics of the candidate events in two bodies.

Channel	Mass [GeV/c^2]	E_B [GeV]	d/σ_d	τ_B [ps]	$\lvert\cos\theta^*\rvert$	Distance in σ from resonant mass
$K\pi$	5.47 ± 0.10	43.7	8.5	1.5	-	-
$\rho\pi$	5.40 ± 0.09	38.1	70.4	3.4	0.68	+0.95
$K^*\pi$	5.21 ± 0.06	40.0	17.6	1.2	0.59	+0.78

The invariant mass distribution for the sum of all the two body channels investigated is given in figure 3. The agreement between real and simulated data in the invariant mass region outside the signal range is good, showing that the effect of the selection cuts is well reproduced in the simulation.

The two candidates with three-prong topology were checked to study their compatibility with a charmed decay channel. The estimated contribution to the background from fully reconstructed $B \to J/\psi K$ and $B \to D^0\pi$ decays is 0.06 events. Furthermore it was found that the particle combination closest to a charm state mass was 5.6 σ from the D^0 mass for the $\rho\pi$ candidate and the corresponding invariant mass of the three-prongs was (5.86 ± 0.10) GeV/c^2 which is incompatible with the B mass.

The number of background events was determined from the sum of all the two body modes considered using both the procedures described above. Using the first method, the background amounts to 0.30 ± 0.17 events. A more accurate estimate was obtained by studying the individual rejection power of the selection cuts. Summing over all the channels considered gives a total background for the two body modes of 0.29 ± 0.07 events which is in agreement with that derived previously, but is more precise. Possible systematics in the background estimation were studied by comparing the ratio of the number of events in the mass interval between 5.1 GeV/c^2 and 5.5 GeV/c^2 in real and simulated data after loosening the cuts on the track impact parameters and on the decay distance and removing the charm rejection. This ratio is sensitive both to systematics on the absolute normalization and to the shape of the invariant mass spectrum. These ratios were found to be consistent with unity for all the decay multiplicities. Nevertheless, due to the limited statistics, systematic effects at the level of 20% could not be excluded. This has been taken into account in the estimate of the uncertainty on the expected number of background events. An additional source of systematic uncertainties comes from decays of b baryons. The fraction of b baryons was increased by 50% by re-weighting the simulated events in which at least one of the tracks used at the secondary vertex originated from a decay of a beauty baryon. The rejection factors were recomputed and the observed 6% increase in the estimated background was also included.

Adding in quadrature the uncertainties on the absolute normalization, the shape of the invariant mass distribution and of the b baryon fraction, the estimated background becomes 0.29 ± 0.09 events. For all three channels with a candidate, no background event is present in the simulated sample in the range $(5.1 - 6.0)$ GeV/c^2. In the real data

sample no entries above 5.0 GeV/c^2 were observed outside the signal region. Using the central value of the background estimation of 0.29 events, the probability that three or more candidates in the signal region all originate from a fluctuation of the background is 3×10^{-3}. After propagation of the error on the background estimate, a final value for this probability of 6×10^{-3} is derived. Upper limits for the branching ratios of the individual channels are given in table 2.

Table 2: Summary of the upper limits at 90 % confidence level for two body decays. The efficiency ϵ quoted refers to the charged particle decay mode that has been searched for. The quoted upper limit (UL) has been corrected for the resonance branching fraction into the final state.

Channel	Events	Bkg.	ϵ [%]	Signal Event UL	Theory BR$\times 10^5$		Exp. UL BR$\times 10^5$		This UL BR$\times 10^5$
$B^0_d \to \pi^+\pi^-$	0	0.04	14	2.3	1.8	[2,3]	2.9	[6]	5.5
$B^0_{d,s} \to K^+\pi^-$	1	0.02	11	3.9	1.1-1.8	[1–3]	2.6	[6]	9
$B^0_{d,s} \to K^+K^-$	0	0.002	5	2.3	-		0.7	[6]	12
$B^0_d \to p\bar{p}$	0	0.001	4	2.3	-		3.4	[16]	35
$B^-_u \to \rho^0\pi^-$	1	0.04	5	3.9	0.4-1.4	[2,3]	15	[17]	26
$B^-_u \to K^{*0}\pi^-$	1	0.02	4	3.9	0.6-0.9	[1,2]	15	[18]	48
$B^-_u \to K^-\rho^0$	0	0.08	4	2.3	.01-.06	[1,2]	8	[18]	19
$B^-_u \to K^-\phi$	0	0.005	3.5	2.3	0.6-1.4	[1,2,4]	9	[18]	44
$B^0_{d,s} \to K^+a^-_1$	0	0.08	3	2.3	-		-		39

3.2 Three body decay modes

Three body charmless modes were studied in the channels:

- $B^-_u \to \pi^-\pi^+\pi^-$
- $B^-_u \to K^-\pi^+\pi^-$
- $B^-_u \to K^-K^+K^-$
- $B^-_u \to p\bar{p}\pi^-$

The $\pi\pi$, $K\pi$ and KK pairs compatible with a ρ, K^* or ϕ were treated as such and have already been discussed in the previous section. Three events were found in the B invariant mass signal region (see figure 4); their characteristics are given in table 3.

Table 3: Characteristics of the candidate events in three bodies.

Channel	Mass [GeV/c^2]	E_B [GeV]	d/σ_d	τ_B [ps]
$\pi\pi\pi$	5.26 ± 0.05	34.6	27.2	2.1
$K\pi\pi$	5.23 ± 0.05	40.8	5.1	2.4
$K\pi\pi$	5.39 ± 0.04	20.3	17.6	3.0

The event in the $\pi\pi\pi$ channel has two tracks with an invariant mass 3.2 σ above the J/ψ mass when assuming them to be muons. In this case a possible interpretation in terms of a fully reconstructed B decay is as a candidate event for the Cabibbo suppressed decay

$B \to J/\psi\pi$, since imposing the kaon mass for the third particle moves the total mass above the B meson mass. For the other two candidates, all two particle combinations are more than 8 σ from charm states.

Table 4: Summary of the 90 % C.L. upper limits for three body decays.

Channel	Events	Bkg.	ϵ [%]	Signal Event UL	Theory BR$\times 10^5$		Exp. UL BR$\times 10^5$		This UL BR$\times 10^5$
$B_u^- \to \pi^+\pi^-\pi^-$	1	0.8	5	3.3	6	[8]	19	[16]	22
$B_u^- \to K^-\pi^+\pi^-$	2	0.7	4	4.7	-		19	[18]	40
$B_u^- \to K^+K^-K^-$	0	0.01	2.5	2.3	-		35	[19]	31
$B_u^- \to p\bar{p}\pi^-$	0	0.02	2.8	2.3	-		16	[20]	50

Due to the higher multiplicity and the lack of intermediate mass constraints, the background in the signal region is larger than in two body decay modes. It has been estimated to be 1.5 events. No significant excess was observed and upper limits are given in table 4.

3.3 Four body decay modes

Four body charmless modes were studied in the channels:

- $B_d^0 \to \pi^+\pi^-\pi^+\pi^-$
- $B_{d,s}^0 \to K^+\pi^-\pi^+\pi^-$
- $B_d^0 \to p\bar{p}\pi^+\pi^-$

The $\pi\pi\pi$ combinations compatible with the a_1 resonance were already discussed in the two body decay section. One event was found in the invariant mass signal region with an estimated background of four events (see figure 5).

Table 5: Characteristics of the candidate event in four bodies.

Channel	Mass [GeV/c^2]	E_B [GeV]	d/σ_d	τ_B [ps]
$\pi\pi\pi\pi$	5.43 ± 0.05	39.6	13.2	1.4

The characteristics of the candidate event are listed in table 5. Upper limits are given in table 6.

Table 6: Summary of the 90 % C.L. upper limits for four body decays.

Channel	Events	Bkg.	ϵ [%]	Signal Event UL	Theory BR$\times 10^5$		Exp. UL BR$\times 10^5$		This UL BR$\times 10^5$
$B_d^0 \to \pi^+\pi^+\pi^-\pi^-$	1	2.1	3.5	2.9	10	[8]	67	[17]	28
$B_{d,s}^0 \to K^+\pi^+\pi^-\pi^-$	0	1.9	2.8	2.3	-		-		21
$B_d^0 \to p\bar{p}\pi^-\pi^-$	0	0.06	1.4	2.3	-		25	[20]	95

4 Conclusions

A search for hadronic charmless decays of B mesons has been performed using 1.6 million hadronic Z^0 decays. Several decay modes in two, three and four body channels were investigated. Three candidates were found in two body modes with an estimated background of 0.29 ± 0.09 events. The probability for a background fluctuation to give three or more events in the signal region was estimated to be 6×10^{-3}. These events are interpreted as a signal of charmless decays of B mesons. In three and four body modes four candidates were found but, due to the increased combinatorial, the estimated background was larger compared to two body modes and no significant excess was observed. Upper limits for the branching ratios in the individual channels are given.

Acknowledgements

We are greatly indebted to our technical collaborators and to the funding agencies for their support in building and operating the DELPHI detector, and to the members of the CERN-SL Division for the excellent performance of the LEP collider.

References

[1] N.G. Deshpande and J. Trampetic, *Phys. Rev.* **D 41** (1990) 895.
[2] L.L. Chau *et al.*, *Phys. Rev.* **D 43** (1991) 2176.
[3] A. Deandrea *et al.*, *Phys. Lett.* **B 320** (1994) 170.
[4] N.G. Deshpande and X.G. He, University of Oregon, Inst. of Theoretical Science Preprint OITS 538 (1994).
[5] R. Ammar *et al.*, CLEO Coll., *Phys. Rev. Lett.* **71** (1993) 674.
[6] M. Battle *et al.*, CLEO Coll., *Phys. Rev. Lett.* **71** (1993) 3922.
[7] M. Bander, D. Silverman and A. Soni, *Phys. Rev. Lett.* **43** (1979) 242.
M. Gronau *et al.*, *Phys. Rev.* **D 50** (1994) 4529.
[8] K. Berkelman, *Hadronic Decays*, in *B Decays* ed. by S. Stone, World Scientific, Singapore 1992.
[9] A.V. Dobrovolskaya *et al.*, *Phys. Lett.* **B 229** (1989) 293.
[10] J. Swain, Northeastern University preprint NUB-3101 (1995).
[11] R. Akers et al., OPAL Coll., *Phys. Lett.* **B 337** (1994) 393.
[12] P. Aarnio *et al.*, DELPHI Coll., *Nucl. Instr. Meth.* **A 303** (1991) 233.
[13] P. Abreu *et al.*, DELPHI Coll., *Phys. Lett.* **B 312** (1993) 253.
[14] P. Abreu *et al.*, DELPHI Coll., *Z. Phys.* **C 65** (1995) 555.
[15] T. Sjöstrand, *Comp. Phys. Comm.* **82** (1994) 74.
[16] D. Bortoletto *et al.*, CLEO Coll., *Phys. Rev. Lett.* **62** (1989) 2436.
[17] H. Albrecht *et al.*, ARGUS Coll., *Phys. Lett.* **B 241** (1990) 278.
[18] P. Avery *et al.*, CLEO Coll., *Phys. Lett.* **B 223** (1989) 470.
[19] H. Albrecht *et al.*, ARGUS Coll., *Phys. Lett.* **B 262** (1991) 148.
[20] C. Bebek *et al.*, CLEO Coll., *Phys. Rev. Lett.* **62** (1989) 8.

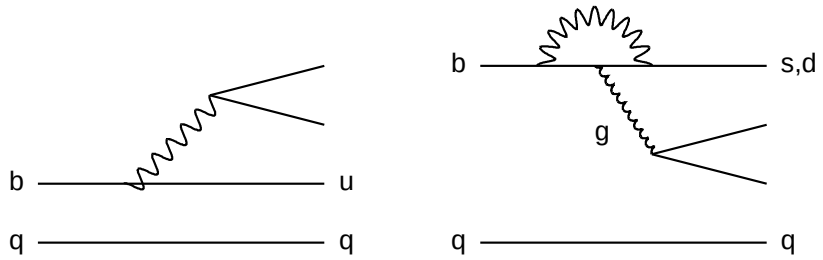

Figure 1: Diagrams for the tree level $b \to u$ (left) and the penguin $b \to s, d\ g$ (right) charmless decays.

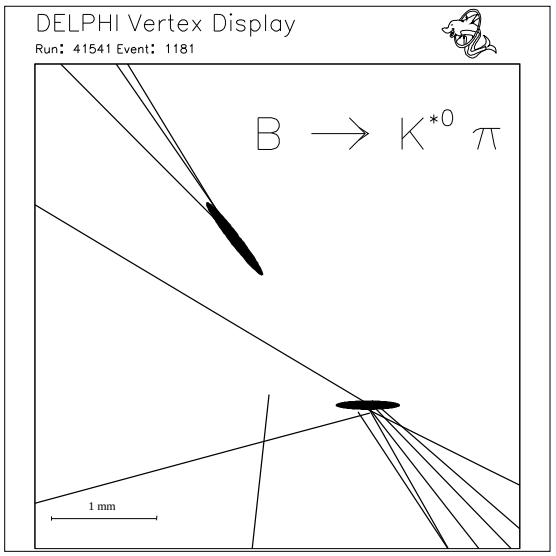

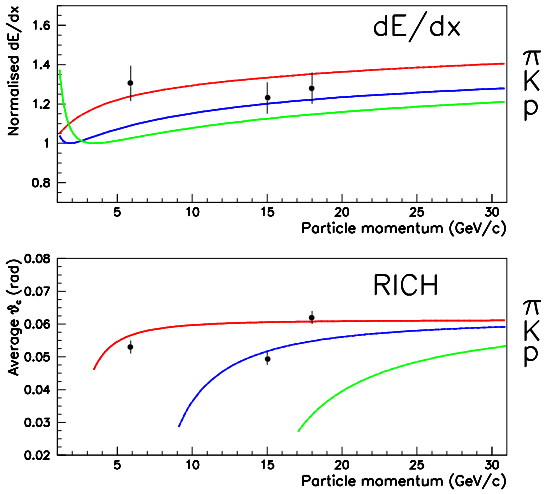

Figure 2: The candidate $B \to K^*(892)\pi$ decay: a magnified view of the extrapolated tracks at the vertex is displayed above. The primary and secondary vertices are indicated by error ellipses corresponding to 3 σ regions. The plot below summarises the hadron identification properties. The lines represent the expected response to pions, kaons and protons and the points with error bars the measured values for the reconstructed B decay products.

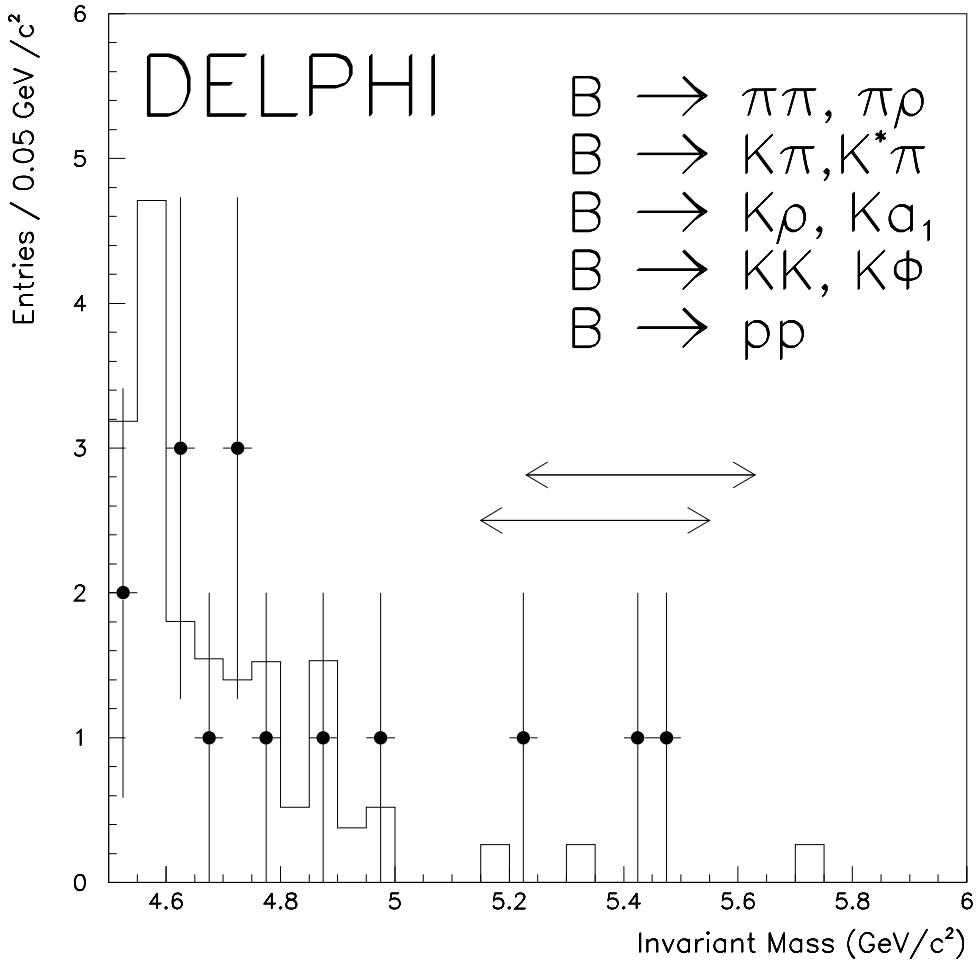

Figure 3: Invariant mass distribution for two body decays. Real data events are indicated by the dots while simulated data are shown by the histogram. The normalization is given by the equivalent number of Z^0 decays. The arrows indicate the signal mass interval for candidate B_d^0 (lower) and B_s^0 (upper).

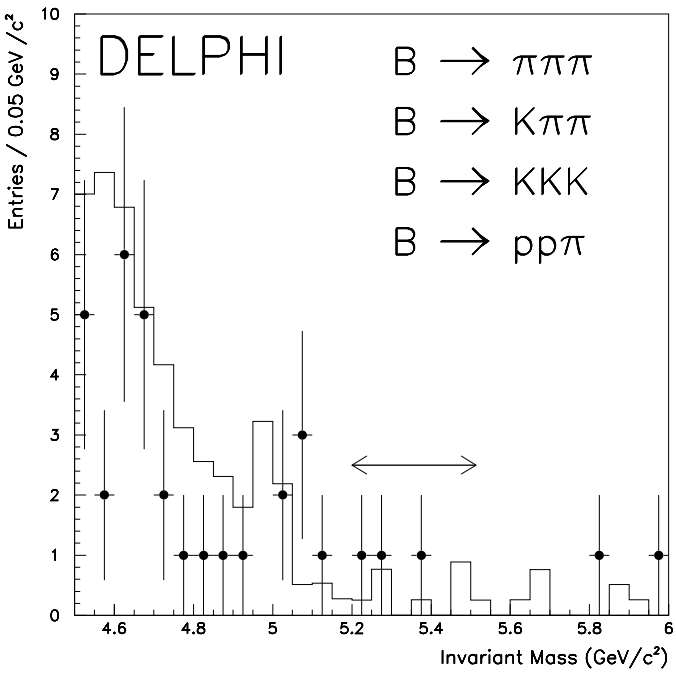

Figure 4: Invariant mass distribution for three body decays for real and simulated data.

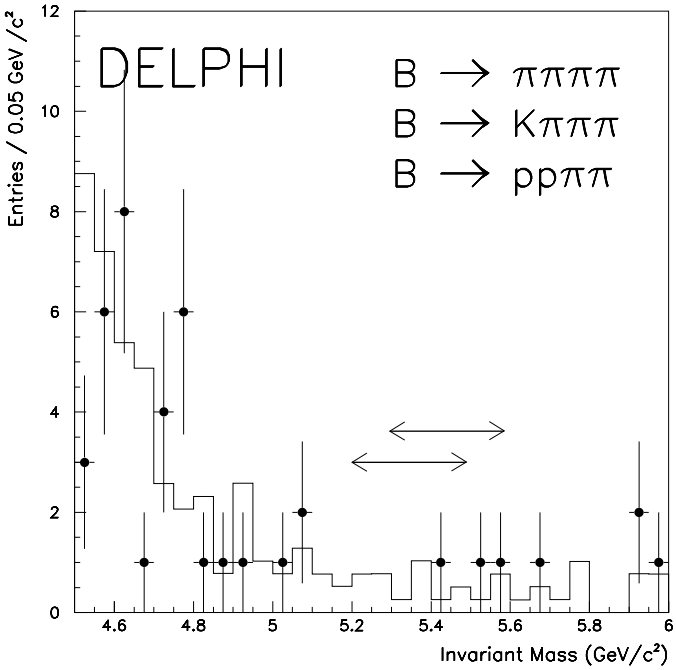

Figure 5: Invariant mass distribution for four body decays for real and simulated data. The arrows indicate the signal mass interval for candidate B_d^0 (lower) and B_s^0 (upper). The two events between 5.5 GeV/c^2 and 5.6 GeV/c^2 are in the $\pi\pi\pi\pi$ channel and thus are not consistent with the B_s^0 hypothesis